Modeling of a Cohesive Granular Materials by a Multi-scale Approach

T. K. Nguyen, G. Combe, D. Caillerie, J. Desrues

UJF-Grenoble 1, Grenoble-INP, CNRS UMR 5521, 3SR Lab., B.P. 53, 38041 Grenoble Cedex 09, France

Abstract. The paper presents a FEM×DEM two-scale modeling of cohesive granular materials. At the microscopic level, a Discrete Element Method (DEM) is used to model the granular structure (rigid disks). At the macroscopic level, the numerical solution of a boundary value problem is obtained via a Finite Element Method (FEM) formulation. In order to bridge the gap between micro- and macro-scale, the concept of Representative Volume Element (REV) is applied: the average REV stress and the consistent tangent operators are obtained in each macroscopic integration point as the results of DEM simulation. The numerical constitutive law is determined through the DEM modeling of the microstructure to take into account the discrete nature of granular materials. The computational homogenization method is first described and then illustrated in the case of a biaxial compression test.

Keywords: Multi-scale, FEM, DEM, homogenization, numerical modeling, cohesive contact law, granular materials.
PACS: 47.11.Fg, 45.70.Cc, 62.20.F-

INTRODUCTION

Granular materials are discrete and heterogeneous. One way to model earth structures with these materials is to use Finite Element Method (FEM), which is based on a continuum media assumption. Unfortunately, this method cannot realistically model the discrete nature of soils. In recent years, many authors have proposed multi-scale approach [1,2,3] to investigate the behavior of materials by using informations from the micro level. By this way, the materials are studied at two different scales. By introducing the response of the grain scale microstructure, a multi-scale approach does not require any phenomenological constitutive law at the continuum scale (FEM-Gauss points).
Based on previous works [4,5], we present in this paper new improvements of our two-scale modeling approach combining FEM at the macro-scale and DEM at the micro-scale.

MULTI-SCALE COUPLING METHOD

A two-scale numerical homogenization approach by FEM-DEM is considered, Figure 1. At the small-scale level (Gauss points), the constitutive equation $\sigma = F(\varepsilon)$ is numerically obtained by a DEM on a Representative Elementary Volume (REV). A gradient displacement tensor is applied to REVs assigned to each Gauss points. The stress response of the REV is computed using the very classical homogenization formula [6] $\sigma_{ij} = \frac{1}{S}.\sum_{c=1}^{N_C} f_i^c . l_j^c$ where S is the volume of the REV (area in 2D). f_i^c and l_i^c are respectively the component *i* of the contact forces acting in contact *c* and the component *j* of the branch vector *l* joining the mass centers of two grains in contact.

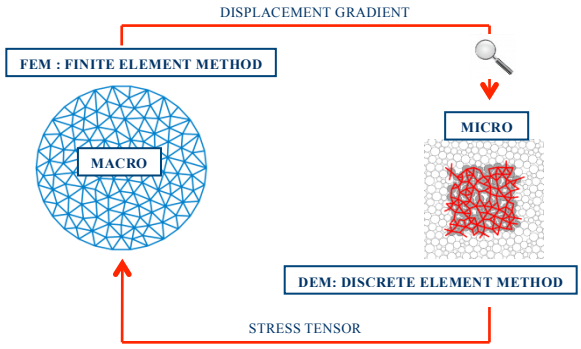

FIGURE 1. Computational homogenization scheme

At the macroscopic level, a numerical solution for the Boundary Value Problem (BVP) is obtained using FEM. To bridge the scales between FEM and DEM, the definition of consistent tangent stiffness matrix C_{ijkl} may be expressed as a function of displacement gradient $d\sigma_{ij} = C_{ijkl}.\frac{\partial du_k}{\partial x_l}$. The upscale technique consists of using the discrete model at each Gauss point of the FEM mesh to derive numerically the constitutive response.

MICRO-SCALE (DEM) MODEL

The numerical model of granular materials behaviour is herein obtained by a classical Discrete Element Method approach (soft-contact dynamics type) using Periodic Boundary Conditions [7] (PBC). A unique Representative Elementary Volume (REV) is associated to each Gauss point. This REV is made of a dense packing of 400 polydisperse disks. All grains interact via linear elastic laws and Coulomb friction when they are in contact [8]. Accordingly, the normal repulsive contact force f_{el} is related to the normal apparent interpenetration δ of the contact as $f_{el} = k_n \cdot \delta$, where k_n is a normal stiffness coefficient ($\delta > 0$ if a contact is present, $\delta = 0$ if there is no contact). The tangential component f_t of the contact force is proportional to the tangential elastic relative displacement, with a tangential stiffness coefficient k_t. In order to model cohesive-frictional granular materials, a local cohesion is introduced at the level of each pair of particles by adding an attractive force f_c to f_{el}; f_c is constant for each contact. The overall normal force for two grains in contact is $f_n = f_{el} + f_c$. The Coulomb condition $\|f_t\| \le \mu . f_{el}$ requires an incremental evaluation of f_t in each time step, which leads to some amount of slip each time one of the equalities $f_t = \pm \mu \cdot f_{el}$ is imposed. In that study, k_n is such that $\kappa = k_n / \sigma_2 = 1000$ [9], where σ_2 is the 2D isotropic pressure. The stiffness ratio is $k_n / k_t = 1$. The adhesion force f_c is defined by reference to the mean level of pressure as suggested by [10]: $p^* = f_c / (a \cdot \sigma_2)$ where a is the typical diameter of grains. So p^* is a ratio scaling the attractive part of the mean stress in the sample with the repulsive part due to particle overlap. Hereafter, $p^* = 1$. The intergranular angle of friction is $\mu = 0.5$.

A degradation of the cohesion is taken into account by considering a vanishing of f_c at a contact when sliding or separation occurs. This correspond to a simple model of granular materials with brittle cemented contacts.

The Figure 2 shows a REV of 400 particles with PBC submitted to a deviatoric loading (biaxial test). The stress-strain response is displayed on the Figure 3. Because this small assembly of discs is initially dense, the volumetric strain is here essentially dilative.

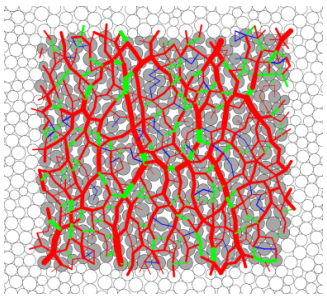

FIGURE 2. A REV of 400 particles with PBC. The contact forces are displayed with the following convention: the width of the lines joining the centers of two particles in contact is proportional to the amplitude of the normal force. Red, green, blue lines distinguish respectively compressive forces with cohesion $(f_n > 0, f_c < 0)$, cohesionless contacts $(f_n > 0, f_c = 0)$ and attractive contacts $(f_n < 0, f_c < 0)$.

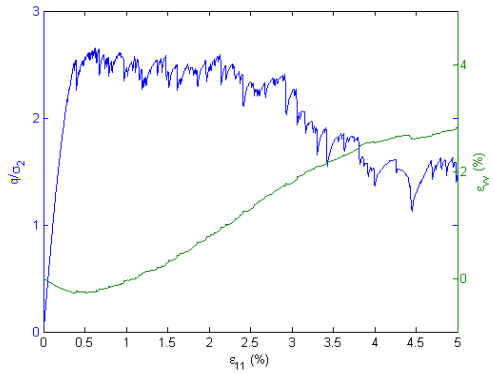

FIGURE 3. Mechanical response of the REV of 400 cohesive-frictional discs submitted to a biaxial loading. The blue curve corresponds to the evolution of the normalized vertical deviatoric stress (q / σ_2) versus the vertical strain ε_{11}. The green curve display $\varepsilon_{vv} = tr\underline{\underline{\varepsilon}}$ evolution along the biaxial compression.

FEM × DEM SIMULATION OF A BIAXIAL COMPRESSION

The FEM×DEM approach was implemented in the FEM code Lagamine [11] that is able to manage large strains. The implementation involved significant modification in the original code, but it essentially consisted in adding the DEM modeling as a constitutive numerical law.

This section presents the results obtained by the FEM×DEM approach for the simulation of a biaxial test (vertical compression at constant strain rate and constant lateral stress) in plane strain conditions. The results presented here were obtained with on a granular sample modeled at the continuous macro-scale by a mesh of 128 finite elements (Q8 –

rectangular elements of 8 nodes) with 4 Gauss integration points, Figure 4. At the start of the computation, the REV is strictly the same for each Gauss point.

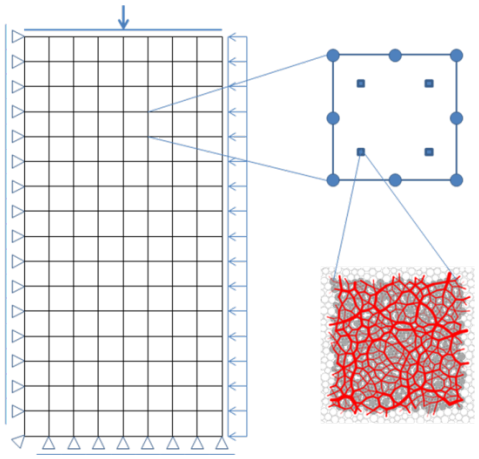

FIGURE 4. Geometry of biaxial test

Macroscopic results

The macroscopic behavior obtained via the FEM×DEM approach is shown on the Figure 5. This mechanical response is typical of that is classically observed on a laboratory drained triaxial test on dense cemented sands, or weak sandstones: from the isotropic state, the deviatoric stress $q = \sigma_1 - \sigma_2$ increases until it reaches a peak corresponding to the maximum strength of the materials. Then, one can observe a softening behavior until the $q = \sigma_1 - \sigma_2$ reach a plateau for large strains. The softening (post-peak response of the specimen) is more pronounced than in purely frictional materials, for two reasons: one is that the degradation of the cohesion comes in addition to the other degradation mechanisms like dilatancy and changes in contact orientation distribution. The second reason is strain localization. It is well known that in FEM modeling, softening constitutive models lead to localization in the response of the BVP. In experimental tests, localization occurs as well. The modeling of strain localization has been a crucial objective in the last three decades. We observe here, not surprisingly, that localization occurs as well in the double-scale FEM × DEM approach. In the Figure 6-left, the local distortion of the mesh shows clearly a shear band in the specimen. This is confirmed on the Fig. 6-right by the map of the second invariant of the strain tensor. Due to localization, the strain process concentrates in this narrow band. A given increment of displacement on the top boundary is no more accommodated by an overall strain in the whole specimen, but by a much faster shear deformation process in the shear band. This is the reason for a much faster softening of the specimen response than the REV response.

[12] shown that mesh-dependency arises for localization process in FEM approach. Other mesh sizes have been tested (not presented here) confirming mesh dependency. A regularization method should be used to restore objectivity in that respect. Enriched media can be considered at the macro-scale, however this question is out of the scope of the present paper.

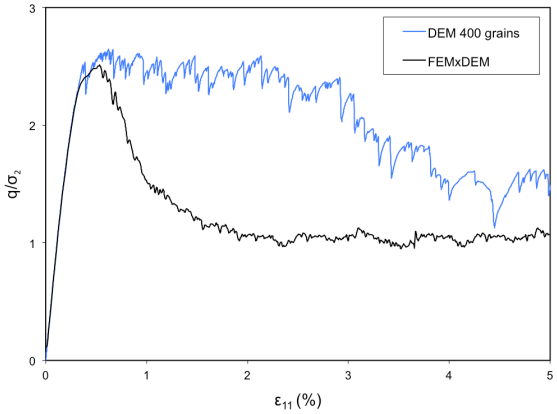

FIGURE 5. Biaxial test response. Comparison of DEM and FEM-DEM methods.

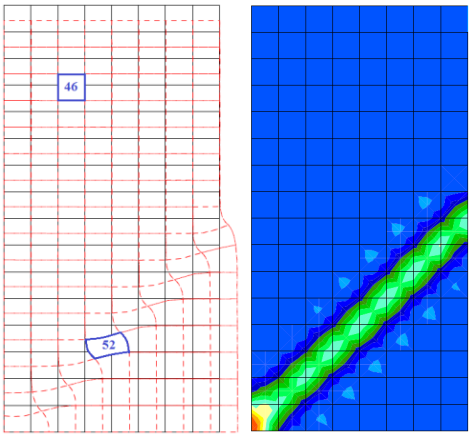

FIGURE 6. Biaxial compression test: deformed structure (left) and map of the second invariant of strain tensor (right) showing shear localization (for $\varepsilon_{11} = 3\%$ of axial strain).

Microscopic Analysis

In this section, we propose to analyze the stress evolution for various Gauss points at different location in the mesh. We focused on the Gauss points of Q8 n°46 and n°52 (see Fig. 6). The element 52 is chosen

in the shear band whereas the element 46 is far from the shear band, in a "homogeneous zone".

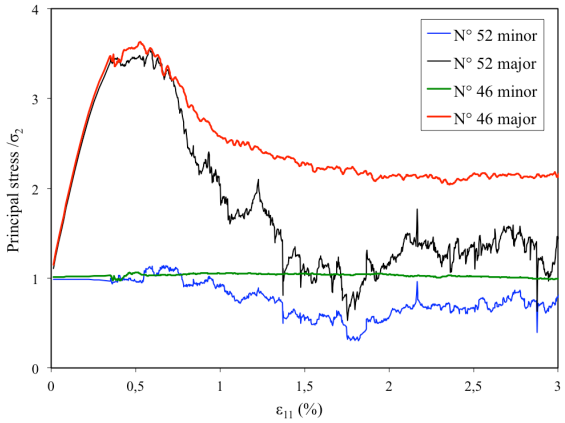

FIGURE 7. Elements 52 and 46, 1st Gauss point: principal stress (minor and major) during the test.

The Figure 7 shows the evolution of Principal Stresses (PS) (minor and major) in the two elements. As for the major PS, we observe that their respective evolutions diverge once the maximum shear strength is reached. The stress variations are rather smooth in element 46 and noisy in 52. Both 46 and 52 show stress reduction, which is consistent with the softening of the specimen as a structure. The minor PS shows the same trend with respect to smoothness. PS directions (not shown here) show erratic values in the shear band. Clearly, the shear band becomes the only active part of the specimen once localization has started; in this active zone, the deformation process is intensive and produces large micro-structural reorganization with severe scattering in the local stress.

CONCLUSION

A two-scale approach to investigate the behavior of cohesive granular materials has been presented, combining DEM at the micro-scale with FEM modeling at macroscopic level. The FEM×DEM mechanical response of a granular material submitted to a biaxial response was analyzed both at the macroscopic and microscopic scales. Strain localization has been observed. Moreover, local stress evolutions have been presented and analyzed. The results obtained allow to validate the approach and open new perspectives. Further developments will concern the use of a second gradient model for the FEM [13] to avoid mesh dependency. Moreover, a "double cohesion scale" model developed to manage assemblies of cemented grains will be used to model sandstones.

ACKNOWLEDGMENTS

This work was carried out as part of GeoBridge research project at 3SR lab, Grenoble, France, which is funded by the French ANR (Agence Nationale de la Recherche).

REFERENCES

1. C. Miehe, J.Dettmar, *Comput. Methods Appl. Mech. Engrg*, 1993 (2004) 225-256.
2. H. A. Meier, P. Steinmann, E. Kuhl, *Technische Mechanik, Band 28, Heft 1,* 2008, 32-42.
3. V. Kouznetsova, W.A.M. Brekelmans, F.P.T. Baaijens, *Computational Mechanics* 27 (2001) 37-48.
4. M. Nitka, G. Bilbie, G. Combe, C. Dascalu, J. Desrues, "A DEM - FEM two scale approach of the behaviour of granular materials" in *Powders and Grains 2009*, Colorado School of Mines, Golden, CO, USA, pp 443-446, 2009
5. M. Nitka, G. Combe, C. Dascalu and J. Desrues, *Granular Matter*, Vol. 13, issue 3, pp 277-281, 2011
6. Weber J., 1966. Recherches concernant les contraintes intergranulaires dans les milieux pulvérulents. *Bul. liaison P. et Ch. N°, juilet–août.*
7. F. Radjaï, F.Dubois, "Discrete-element Modeling of Granular Materials", John Wiley & Sons, Inc. 2011.
8. P. A. Cundall, O. D. L. Strack, "A discrete numerical model for granular assemblies" in *Geotechnique*, 29(1):47-65, 1979.
9. Combe, G., Roux, J-N., "Discrete numerical simulation, quasistatic deformation and the origin of strain in granular materials" in *3rd International Symposium on Deformation Characteristics of Geomaterials,* Lyon, France, pp. 1071-1078, 2003.
10. F. Gilabert, J-N. Roux, A. Castellanos, "Computer simulation of model cohesive powders: influence of assembling procedure and contact laws on low consolidation states" in *Physical Review E*, Vol. 75, 011303, 2007.
11. Lagamine code, University of Liège, Belgium.
12. Matsushima T., Chambon R., Caillerie D. (2002), *Int. Journal for Numerical Methods in Engineering vol.54 No 4*, pp. 499-521
13. Chambon, R., Caillerie, D. and Matsushima, T., *Int. Journal of Solids and Structures 38* 8503-8527.